Proceedings of the ASME 2017 Dynamic Systems and Control Conference
DSCC2017
October 11-13, 2017, Tysons, Virginia, USA

DSCC2017-5194

A FRAMEWORK OF CONTROL-ORIENTED REACTION-BASED MODEL FOR TRAJECTORY-BASED HCCI COMBUSTION WITH VARIABLE FUELS

Chen Zhang[a], Zongxuan Sun[b]
Department of Mechanical Engineering
University of Minnesota, Twin Cities Campus
Minneapolis, MN 55455

ABSTRACT

A novel combustion control, i.e. the trajectory-based combustion control, was proposed previously. This control is enabled by free piston engines (FPEs) and utilizes the FPE's controllable piston trajectory to enhance thermal efficiency, reduce emissions and realize variable fuels applications. On top of that, a control-oriented model was also developed aimed to implement the trajectory-based combustion control in real-time. Specifically, a unique phase separation method was proposed in the model, which separates an engine cycle into four phases (pure compression, ignition, heat release and pure expansion) and employs the minimal reaction mechanism accordingly. In this paper, the framework of the previous control-oriented model is extended to variable fuels, such as methane, n-heptane and bio-diesel. Such an extension is reasonable since the separated four phases are representative in typical combustion processes of all fuels within an engine cycle. Besides, a least-squares optimization is formulated to calibrate the chemical kinetics variables for each fuel. At last, simulation results and the related analysis show that all the derived control-oriented models have high fidelity and much lighter computational burdens to represent the HCCI combustion of each fuel along variable piston trajectories.

INTRODUCTION

How to reduce fuel consumption and emissions simultaneously becomes a key challenge for all the automotive engineers. In order to overcome the challenge, homogeneous charge compression ignition (HCCI) combustion has been proposed [1-3]. However, the mass application of HCCI technology has yet to be achieved, which is mainly caused by the lack of adequate control means in the conventional internal combustion engine (ICE) to adjust the HCCI combustion over the entire operating range. As shown in Fig. 1, the HCCI combustion process is determined by the interaction between the chemical kinetics and the in-cylinder gas dynamics in a feedback manner. The existing control methods in conventional ICEs, such as regulating exhaust gas recirculation (EGR) [4, 5], variable valve timings [6, 7] and stratifying charge [8, 9], can only affect the dynamic interaction cycle-by-cycle, which limits the control effects on the entire combustion process.

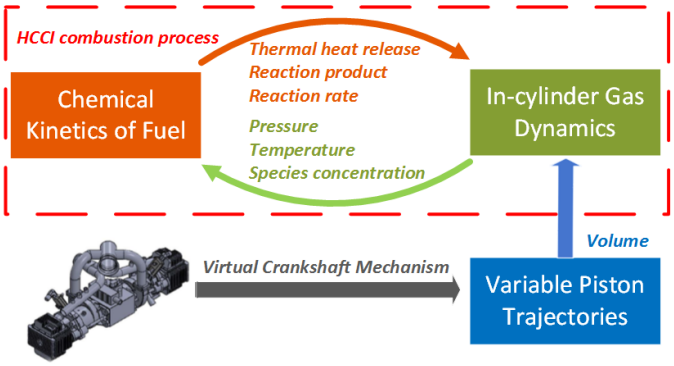

Figure 1. Interaction between chemical kinetics and gas dynamics

A new combustion control, namely the trajectory-based combustion control, was then proposed, which enables a real time control of the HCCI combustion or other low temperature combustion modes [10-12]. This method is realized by free piston engines (FPEs), whose piston motion can move freely in one direction due to the absence of the crankshaft mechanism [13]. Consequently, the FPE enables variable compression ratio (CR) control with potentially higher thermal efficiency and ultimate fuel flexibility [14]. However, the freedom of the piston also raises an issue on its motion control. The "virtual crankshaft" mechanism was then developed, which ensures the piston tracking any desired reference precisely [13, 15]. In this

[a] Email: zhan2314@umn.edu
[b] Corresponding author, Email:zsun@umn.edu, Tel: 612-625-2107

way, the variable piston trajectory in the FPE becomes a new control variable adjusting the gas pressure-temperature history and species concentration through the entire combustion and optimizing the related chemical reactivity and heat transfer process (Fig. 1). The effectiveness of the control method has been demonstrated by extensive simulation studies [10-12, 16].

The overall control system configuration of the trajectory-based combustion control is then shown in Fig. 2. The inner loop is the piston motion control, which is achieved through the "virtual crankshaft" mechanism [13], and the outer loop is the trajectory optimization generating the optimal trajectory reference for the inner loop.

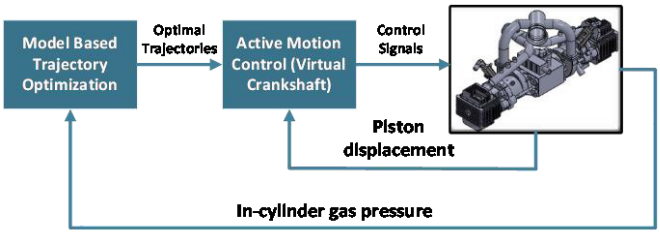

Figure 2. Overall control system configuration

Obviously, a comprehensive reaction-based model with detailed reaction mechanism is not suitable for control due to its heavy computational burden and intrinsic high order. However, existing control-oriented models are also inappropriate due to their over-simplifications on the chemical kinetics [17-20]. Thus, a new control-oriented model with short computation time and sufficient chemical kinetics information is needed.

Such a model was developed recently [21]. In order to satisfy the above requirements, a unique phase separation method is also developed, which separates an engine cycle into four phases, i.e. pure compression, ignition, heat release and pure expansion, and employs minimal reaction mechanisms accordingly. Since the HCCI combustions of all fuels include these four phases, the related model approach can form a framework and be easily extent to other fuels, as long as the chemical kinetics variables are calibrated correctly. Considering the fact that the FPE possesses the ultimate fuel flexibility due to its variable CR, the framework of the control-oriented model makes it convenient for further investigation of the trajectory-based combustion control on variable fuels.

The rest of the paper is organized as follow: The modeling approach of the control-oriented model is briefly described at first. Then, a least squares optimization, aimed to calibrate the chemical kinetics parameters for three different fuels, i.e. methane, n-heptane and bio-diesel, is formulated. Simulation results of the three derived control-oriented models as well as the related discussion, are presented subsequently. The advantages of the proposed framework are concluded at last.

MODEL APPROACH

The modeling approach of the control-oriented model is briefly described in this section, while the details can be found in [21]. Generally, the model consists of three components: a new mechanism producing variable piston trajectories, a physics-based model describing the in-cylinder gas dynamics and a reaction mechanism representing the chemical kinetics.

A. Variable Piston Trajectories

As mentioned in [21], in order to describe variable piston trajectories in a FPE, a new mechanism is developed to represent the piston motion as the x-axis displacement of a point moving around an ellipse in the Cartesian coordinate (Fig. 3).

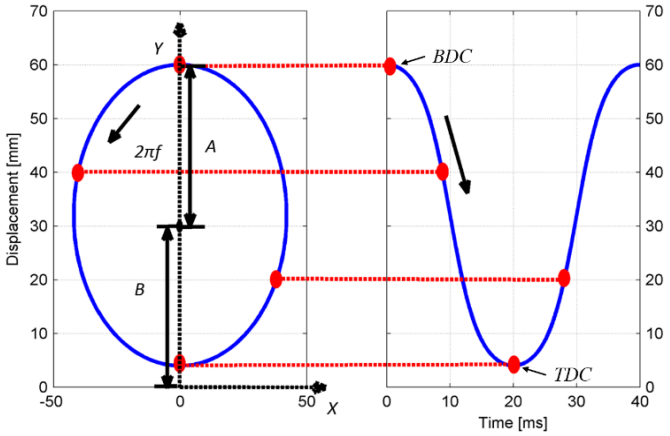

Figure 3. Description of FPE piston motions

The corresponding piston trajectories S can be derived as:

$$S = \frac{A \cdot \Omega \cdot \cos(2\pi f \cdot t)}{\sqrt{\Omega^2 \cdot \cos(2\pi f \cdot t)^2 + \sin(2\pi f \cdot t)^2}} + B \qquad (1)$$

where A is the major axis of the ellipse, B is the location of the ellipse center, f represents the frequency of the engine operation, Ω (= minor axis / major axis) implies the shape of the ellipse and t stands for the time.

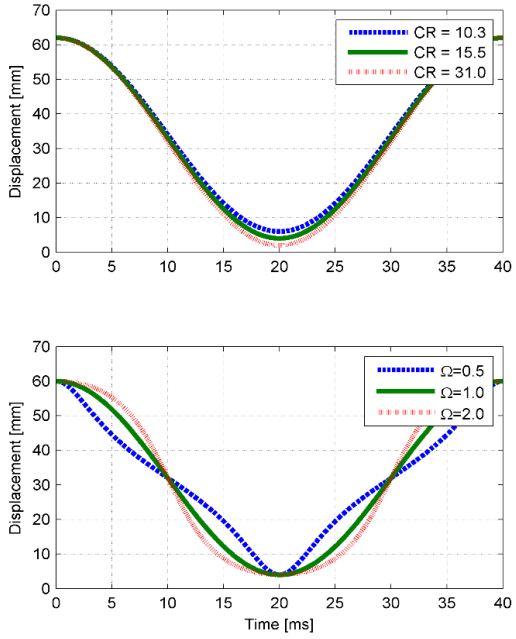

Figure 4. Piston trajectories with different CR (top) and Ω (bottom)

Fig. 4 shows the derived piston trajectories with various CRs and different piston motion patterns between the top dead center (TDC) and the bottom dead center (BDC) points. It has been shown that the FPE enables significant improvements on engine efficiency and emissions simultaneously by implementing specific piston trajectories accordingly [10-12].

B. Physics-based Model

The physics-based model is developed based on the first law of thermodynamics applied to a closed system [21]. The states include pressure P, temperature T and each species concentration $[X_i]$ inside the reaction mechanism.

Pressure rate equation

From the idea gas law, the pressure P and its time derivative is: (R is the universal gas constant)

$$P = \sum_i [X_i] \cdot R \cdot T \tag{2}$$

$$\dot{P} = P \cdot \sum_i [\dot{X}_i] / \sum_i [X_i] + P \cdot \dot{T} / T \tag{3}$$

Temperature rate equation

The rate equation for the in-cylinder gas temperature T is derived based on the first law of the thermodynamics for a closed system and the ideal gas law:

The first law of the thermodynamics for a closed system is:

$$\frac{d(mu)}{dt} = -\dot{Q} - \dot{W} = -\dot{Q} - P\dot{V} \tag{4}$$

where m is the total mass in the cylinder, u is the specific internal energy of the in-cylinder gas, $\dot{Q}$ is the heat transfer rate and $\dot{W}$ is the expansion work rate.

Furthermore, the heat transfer process is assumed as a convection process and the heat transfer coefficient is determined by a modified Woschini correlation [22].

Now, given the fact that the specific enthalpy h can be obtained from the specific internal energy u, the following equation can be achieved:

$$\frac{d(m \cdot h)}{dt} = \dot{P} \cdot V - \dot{Q} \tag{5}$$

On the other hand, the total enthalpy of the in-cylinder gas can also be derived via the sum of each species enthalpy:

$$m \cdot h = \sum_i N_i \cdot \hat{h}_i \tag{6}$$

where N_i is the moles number of species i and $\hat{h}_i$ is mole-based specific enthalpy of species i.

By representing $\hat{h}_i$ from the mole-based constant pressure heat capacity $c_{p,i}(T)$, the time differential of the total enthalpy is:

$$\begin{aligned} \frac{d(m \cdot h)}{dt} &= \sum_i \left(\frac{dN_i}{dt} \cdot \hat{h}_i\right) + \sum_i \left(\frac{d\hat{h}_i}{dt} \cdot N_i\right) \\ &= V \cdot \sum_i ([\dot{X}_i] \cdot \hat{h}_i) + \dot{V} \cdot \sum_i ([X_i] \cdot \hat{h}_i) + V \cdot \dot{T} \cdot \sum_i ([X_i] \cdot c_{p,i}(T)) \end{aligned} \tag{7}$$

Combining (3), (5) and (7), the temperature rate, $\dot{T}$ is derived eventually:

$$\dot{T} = \frac{-\sum_i ([\dot{X}_i] \cdot \hat{h}_i) - \dot{V} \cdot \sum_i ([X_i] \cdot \hat{h}_i)/V + P \cdot \sum_i [\dot{X}_i] / \sum_i [X_i] - \dot{Q}/V}{\sum_i ([X_i] \cdot c_{p,i}(T)) - P/T} \tag{8}$$

C. Chemical Kinetics

The chemical kinetics part of the model mainly offers two critical information from the specific reaction mechanism [21].

Frist, the thermodynamic properties of each species, such as $c_{p,i}$ and $\hat{h}_i$, are produced in the reaction mechanism via the NASA polynomial parameterization [23].

In addition, the history of each species concentration $[X_i]$ is derived via integrating the following differential equation:

$$[\dot{X}_i] = \frac{d}{dt}\left(\frac{N_i}{V}\right) = \frac{\dot{N}_i}{V} - \frac{\dot{V}N_i}{V^2} = w_i - \frac{\dot{V}}{V}[X_i] \tag{9}$$

where w_i is the production rate of species i from the reaction.

In order to reduce the computational burden and keep sufficient chemical kinetics information, an engine operation cycle is separated into four phases (Fig. 5) and in each phase, a specific reaction mechanism with the minimal size is applied to predict the combustion process as precisely as possible:

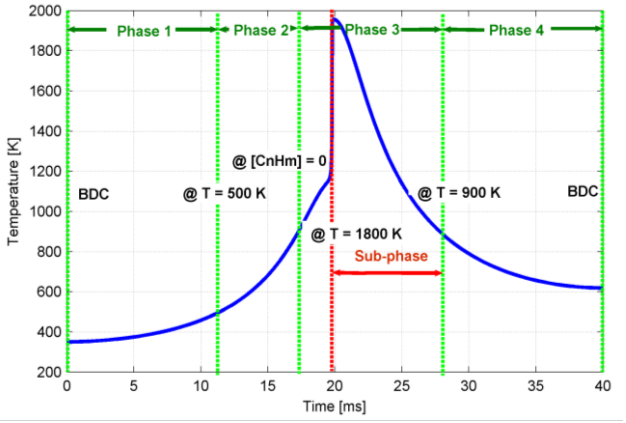

Figure 5. Phase separation within an engine cycle

Phase 1 (pure compression): this phase begins when piston locates at the BDC and ends when T reaches 500K. During this period, few chemical reactions occur due to the low temperature and therefore, no reaction mechanisms need to be applied here.

Phase 2 (ignition): A single reaction step will be employed in this phase to represent the ignition process of the fuel until all the fuel molecules are converted to intermediate species, such as CO and H_2:

$$R_1 : C_nH_m + (n/2)O_2 \rightarrow nCO + (m/2)H_2$$

where its reaction rate is determined by an Arrhenius equation:

$$RR_1 = A_1 \cdot [C_nH_m]^{n_1} \cdot [O_2]^{n_2} \exp\left(-\frac{E_{A1}}{T}\right) \tag{10}$$

where A_1 is the pre-exponential term, n_1, n_2 are the power numbers related to the reactants, and E_{A1} is the activation energy. Intuitively, all three parameters need to be calibrated based on the chemical kinetics of the utilized fuel.

The production rates of each species in this phase are:

$$\begin{cases} w_{C_nH_m} = -RR_1 \\ w_{O_2} = -(n/2)\cdot RR_1 \\ w_{H_2} = (m/2)\cdot RR_1 \\ w_{CO} = n\cdot RR_1 \\ w_{CO_2} = 0 \\ w_{H_2O} = 0 \end{cases}$$

Phase 3 (heat release): afterwards, the intermediate species CO and H_2 will react to generate final products CO_2 and H_2O as well as the major heat release. The corresponding reaction mechanism utilized in this phase is shown as below:

$$R_2 : CO + H_2O \rightarrow CO_2 + H_2$$
$$R_3 : H_2 + 0.5O_2 \rightarrow H_2O$$

where the reaction rates for both reaction steps are determined respectively:

$$RR_2 = A_2 \cdot [CO]^{n_3} \cdot [H_2O]^{n_4} \exp(-\frac{E_{A2}}{T}) \quad (11)$$

$$RR_3 = A_3 \cdot [H_2]^{n_5} [O_2]^{n_6} \exp(-\frac{E_{A3}}{T}) \quad (12)$$

where A_2, A_3, n_3, n_4, n_5, n_6. E_{A2} *and* E_{A3} are the chemical kinetics parameters for these two reaction steps respectively, which are required to be calibrated according to the specific utilized fuel.

Similarly, the production rates of each species in this phase are the sum of all involved reaction rates:

$$\begin{cases} w_{CH_4} = 0 \\ w_{O_2} = -0.5RR_3 \\ w_{H_2} = RR_2 - RR_3 \\ w_{CO} = -RR_2 \\ w_{CO_2} = RR_2 \\ w_{H_2O} = -RR_2 + RR_3 \end{cases}$$

Sub-phase (NOx generation): when the temperature is over 1800K, the production of NOx is significant. The thermal NOx generation mechanism [24] is added here since it is the most suitable mechanism for high temperature and rich oxygen environment. Specifically, Bowman et al have claimed that the thermal generation of NOx is almost exclusively determined by temperature [25]. Therefore, the chemical kinetics of the NOx generation can be assumed to be independent from the utilized fuel. By kinetic analysis, an overall expression for the rate of thermal NOx formation for all the fuels cases is derived [25]:

$$w_{NO_x} = \frac{2.0\times10^{15}}{T^{0.5}}[N_2][O_2]^{0.5} \exp(\frac{-69090}{T}) \quad (13)$$

Phase 4 (pure expansion): after the in-cylinder temperature T decreases to 900K, almost all the reaction products remain constants. Therefore, the rest of the cycle will be simulated as ideal expansion process with the heat transfer until the piston reaches the BDC.

To summarize, the phase separation method transforms the entire chemical kinetics of the HCCI combustion into a sequence based on the thermal state. Such a sequence guarantees the specific chemical kinetics in each phase has little effects on the simulation of the others. As a result, by applying the specific reaction mechanism in each phase, the proposed model not only increases the computational speed by avoiding computing the entire chemical kinetics simultaneously, but also reduces the order of the control-oriented model, which facilitates the subsequent optimization process.

By now, the complete state space of the control-oriented model, e.g. pressure P, temperature T and each species concentration $[X_i]$, has been derived through (3), (8) and (9).

MODEL CALIBRATION FOR VARIABLE FUELS

In order to apply the framework of the control-oriented model to variable fuels applications, the related parameters in the chemical kinetics part need to be calibrated based on the utilized fuel properties. Such a calibration process is presented herein, which generates three control-oriented models for methane, n-heptane, and bio-diesel respectively.

At first, a sensitivity analysis is conducted to identify the most significant parameters in the chemical kinetics part of the model. Afterwards, the selected parameters are calibrated using the simulation results of a comprehensive reaction-based model. In order to further enhance the fidelity of the derived control-oriented model, all the employed comprehensive reaction-based models include the most widely-used detailed reaction mechanisms for the specific fuel respectively. The entire calibration is then achieved by solving a least-squares optimization problem, whose objective function is determined by in-cylinder temperature history, in-cylinder pressure history, and indicative output work. The formulation of the least-squares optimization will be presented at last.

A. Sensitivity Analysis

As can be seen from the model approach, there are total 12 unknown parameters (A_1, A_2, A_3, n_1, n_2, n_3, n_4, n_5, n_6, E_{A1}, E_{A2} *and* E_{A3}) in the chemical kinetics part. Calibrating all of them is not only difficult (generating a high-order optimization problem), but also unnecessary (some unknown parameters may have little effects on the final result). Thus, the parameters that exert the most influence on model response should be identified at first through a sensitivity analysis [26].

In this study, the one-at-a-time method is used. Conceptually, this method proceeds via repeating the model simulation several times, while varying one parameter at a time and holding the others fixed. A sensitivity coefficient can then be calculated by quantifying the corresponding variation of the model output over the perturbation of the specific parameter.

To be more specific, suppose there are n parameters to be calibrated, then the sensitivity coefficient of system response η to parameter β_i can be approximated as:

$$s_i = \beta_i \frac{\partial \eta}{\partial \beta_i} = \beta_i \frac{\eta(\beta_1,\ldots,(1+\delta)\beta_i,\ldots\beta_n) - \eta(\beta_1,\ldots,\beta_i,\ldots\beta_n)}{(1+\delta)\beta_i - \beta_i} \quad (14)$$

where δ is the relative perturbation, whose value is chosen to be 0.01. The system response η in this study is the in-cylinder temperature since it is the most critical parameter for the chemical kinetics analysis.

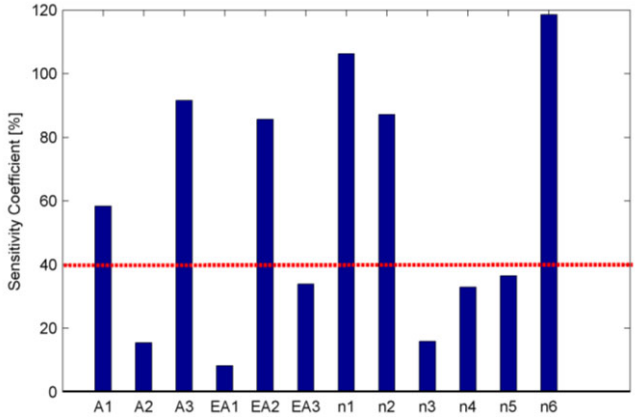

Figure 6. Sensitivity coefficients for all the 12 parameters.

Fig. 6 shows the sensitivity coefficients of all the 12 parameters in the chemical kinetics part of the control-oriented model. All the sensitivity coefficients are first averaged within the engine cycle and then normalized with respect to the mean value of the non-perturbation cylinder temperature. As can be seen, the six parameters, A_1, A_3, n_1, n_2, n_6, *and* E_{A2}, provide more influence on the result. Thus, these six parameters are selected to be calibrated according to the different fuels, while the others are kept fixed as shown in Table 1.

Table 1. Chemical kinetics parameters that are kept constant [27]

Parameters	*Value*
A_2	2.75e7
E_{A1}	15095
E_{A3}	17609
n_3	1
n_4	1
n_5	1

B. Detailed Reaction-based Model

In order to proceed the calibration, reliable results representing the HCCI combustion of each fuel along variable piston trajectories are required. In this study, such reliable results are obtained through the simulation of the detailed reaction-based model of each fuel [10].

Similarly, these detailed reaction-based models also comprise three parts: a mechanism synthesizing variable piston trajectories, a physics-based model representing FPE operation and a specific reaction mechanism. However, those reaction mechanisms include all the elementary reactions affecting the combustion process and capture the entire chemical kinetics, such as the pyrolysis of fuel molecules, the accumulation of free radical species and the generation of final products. Table 2 lists the detailed reaction mechanisms utilized in this study. Their effectiveness, in terms of predictions of ignition delay time and flame propagation speed, have been experimentally validated by different facilities, e.g. shock tube, constant volume chamber, and test-bed engine.

Table 2. Selected detailed reaction mechanisms for calibration

Fuel	# of species	# of reactions	Mechanism
Methane	53	325	GRI-30[a]
n-Heptane	76	366	UW-Madison
Biodiesel	118	1178	LLNL[b]

a: GRI-30 mechanism is mainly proposed by UC Berkeley
b: LLNL stands for Lawrence Livermore National Laboratory

C. Least-Squares Optimization

An automated optimization algorithm is developd to obtain the optimal calibration results. The algorithm is to convert the parameters calibration into a nonlinear least-squares curve fitting problem [28, 29]. The objective function can be formulated as below, enabling handle several simulation data sets using a single vector of the calibration parameters:

$$\min_x \left\| f(x) \right\|^2 = \min_x \left[f_1(x)^2 + \ldots + f_n(x)^2 \right] \quad (15)$$

In this study, 15 simulation data sets (n = 15) are selected for the objective function to ensure that the final result is suitable for the simulations along different piston trajectories. Specifically, the 15 simulation data sets include three groups of piston trajectories. In each group, five piston trajectories share with the fixed CR but variable Ω in the range of 0.5 to 2.0.

Besides, the individual cost function *f(x)* is in the form:

$$f(x) = \begin{bmatrix} W_P\left(\dfrac{P(x) - P_{sim}}{P_{ave}}\right) \\ W_T\left(\dfrac{T(x) - T_{sim}}{T_{ave}}\right) \\ W_w\left(\dfrac{W(x) - W_{sim}}{W_{sim}}\right) \end{bmatrix} \quad (16)$$

and x is the vector of all the parameters to be calibrated:

$$x = \begin{bmatrix} A_1 \\ A_3 \\ E_{A2} \\ n_1 \\ n_2 \\ n_6 \end{bmatrix} \quad (17)$$

Specifically in (16), *P(x), T(x), W(x)* are derived pressure history, temperature history, and indicative output work respectively from the control-oriented model after applying *x* into it. P_{sim}, T_{sim}, *and* W_{sim} are related counterparts from the simulation of the comprehensive reaction-based model. In addition, P_{ave} and T_{ave} are the mean values of the pressure history and temperature history from the comprehensive reaction-based model. The P_{ave} and T_{ave}, as well as the W_{sim}, are utilized as the normalizing factors. At last, W_p, W_t, and W_w are weighting factors, whose values are listed in Table 3.

Table 3. Weighting factors in the cost function *f(x)*

Weighiting factors	*Value*
W_p	0.15
W_t	0.9
W_w	0.6

SIMULATION RESULTS AND DISCUSSION

A. Methane

Obviously, the chemical formula of the methane is CH_4. Therefore, the chemical kinetics part of the control-oriented model for methane, especially its ignition phase, can be further refined as:

$$R_1 : CH_4 + 0.5O_2 \rightarrow CO + 2H_2$$

and the corresponding production rate of each species are:

$$\begin{cases} w_{CH_4} = -RR_1 \\ w_{O_2} = -0.5RR_1 \\ w_{H_2} = 2RR_1 \\ w_{CO} = RR_1 \\ w_{CO_2} = 0 \\ w_{H_2O} = 0 \end{cases}$$

By applying the aforementioned least-squares optimization method, the final calibration results of the control-oriented model for methane are listed in Table 4.

Table 4. Calibration result of the chemical kinetics parameters for the control-oriented model of methane

Parameters	*Value*
A_1	3.734e9
A_3	1.576e9
E_{A2}	9939
n_1	0.54
n_2	1.05
n_6	0.52

The performance of the control-oriented model of methane is then compared with the related reaction-based model in terms of the computational cost and the accuracy of the prediction.

I. Computational Cost

In order to achieve a fair comparison, all the simulations of are conducted using a laptop with 2.60GHz Inter(R) Core ™ i5-3230M processor and 4.00 GB installed memory. As shown in Table. 5, the detailed reaction-based model needs 2070ms to simulate an engine cycle, while the control-oriented model spends only 98ms. In other words, attributed to the unique phase separation method, the computational time of the control-oriented model is reduced by 95.27%.

Table 5. Comparison of the computational times of the two models

Utilized model	**Computational time [ms]**
Detailed reaction-based model	2070
Proposed control-oriented model	98

II. Accuracy of the Prediction

Another comparison between these two models benchmarks the accuracy of the models' response in terms of in-cylinder gas temperature profiles and NOx productions.

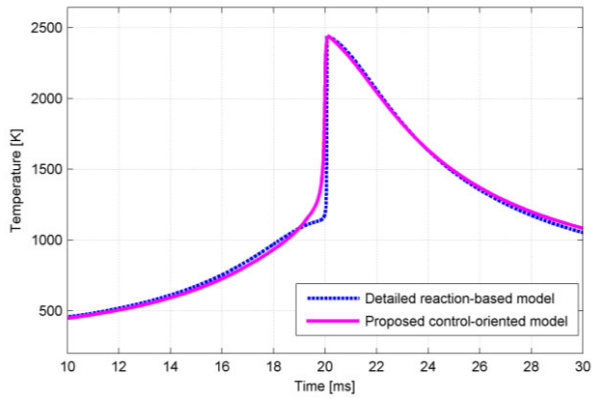

Figure 7. Comparison of temperature profiles between the two models (AFR = 2, CR = 31 and Ω =1.25)

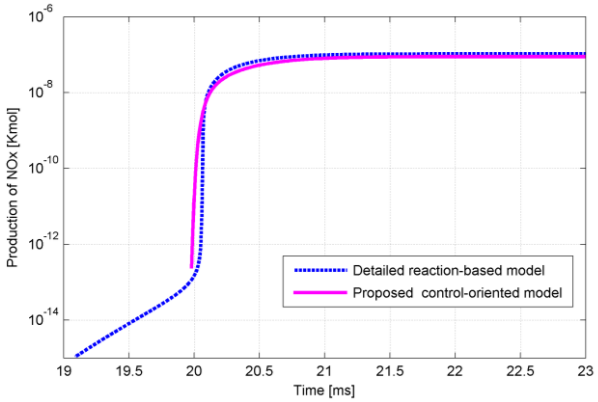

Figure 8. Comparison of NOx production between the two models (AFR = 2, CR = 31 and Ω =1.25)

As shown in Fig. 7 and Fig. 8, at a specific working condition (AFR = 2, CR = 31 and Ω =1.25), both the in-cylinder temperature profiles and the NOx emission produced from the proposed control-oriented model have a good agreement with the results from the detailed reaction-based model. In this way, the effectiveness of the phase separation method has been clearly demonstrated.

Besides, even though the NOx generation is only considered after the T reaches 1800K in the control-oriented model, the final production of NOx still resembles the outcome of the detailed reaction-based model. This phenomenon attributes to two characteristics of the thermal NOx mechanism: 1. the major production of the NOx can be decoupled from the general combustion processes; 2. the chemical kinetics of the thermal NOx mechanism is solely dominated by the T [29].

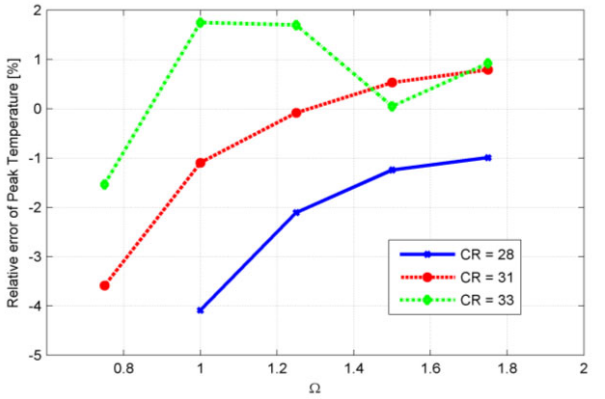

Figure 9. Relative error of peak temperature from the two models at various working conditions

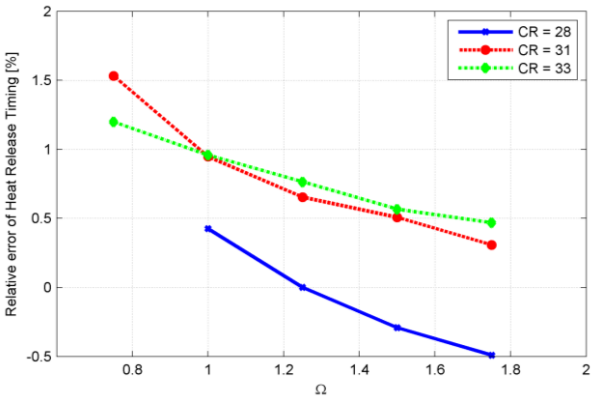

Figure 10. Relative error of time instants of heat release from the two models at various working conditions

In addition, since the calibration takes multiple simulation data sets into account, the fidelity of the control-oriented model should be sustained along different piston trajectories. The corresponding simulation results are shown in Fig. 9 and Fig. 10, which illustrate the relative errors of the peak T and the time instant of major heat release between the two models, respectively. These two characters are selected due to their critical influence on the T profile, the related NOx emission, and the output work. As can be seen from Fig. 9, the relative errors of the peak T between the two models are within the range of -5% to 2%. In addition, the relative errors of the time instant of major heat release are even further smaller, only in the range of -0.5% to 1.5%. Both figures show that the derived control-oriented model for the methane can predict its HCCI combustion accurately at multiple working conditions. It should be noted that when CR = 28 and Ω = 0.75, no combustion occurs from both models.

B. n-heptane

Similarly, the chemical formula of the n-heptane is C_7H_{16} and the related chemical kinetics part is refined as:

$$R_1 : C_7H_{16} + 3.5O_2 \rightarrow 7CO + 8H_2$$

the production rates of each species in the ignition phase are:

$$\begin{cases} w_{C_7H_{16}} = -RR_1 \\ w_{O_2} = -3.5RR_1 \\ w_{H_2} = 8RR_1 \\ w_{CO} = 7RR_1 \\ w_{CO_2} = 0 \\ w_{H_2O} = 0 \end{cases}$$

The final calibration results of the control-oriented model for the n-heptane are listed in Table 6.

Table 6. Calibration result of the chemical kinetics parameters for the control-oriented model of n-heptane

Parameters	*Value*
A_1	1.052e9
A_3	3.726e9
E_{A2}	26981
n_1	-0.12
n_2	0.23
n_6	0.81

Two aspects, i.e. the computational cost and the accuracy of the prediction, are still compared to the two models.

I. Computational Cost

In this case, the detailed reaction-based model needs 3651ms to simulate an engine cycle. Meanwhile, the control-oriented model only spends 102ms, which is comparable to the control-oriented model's computational time for the methane (Table 5). Clearly, the control-oriented model speeds up about 97.21% and thus, the speed advantage of the unique phase separation method is further enhanced.

Table 7. Comparison of the computational times of the two models

Utilized model	**Computational time [ms]**
Detailed reaction-based model	3651
Proposed control-oriented model	102

II. Accuracy of the Prediction

Since the NOx emission is mainly determined by the *T*, the comparisons of the model prediction between the two models are only referred to the *T* in the rest of the paper.

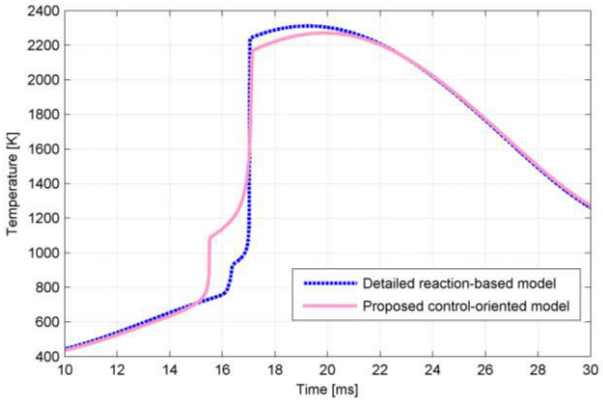

Figure 11. Comparison of temperature profiles between the two models (AFR = 2, CR = 13 and Ω = 1.75)

Fig. 11 shows the comparison of the *T* profiles between the two models for the n-heptane at a specific working condition (AFR = 2, CR = 13 and Ω = 1.75). Clearly, the *T* profiles still possess good agreement, even though the time instant of the start of combustion and the peak temperature differ a little bit (relatively errors are -0.12% and -1.22% respectively).

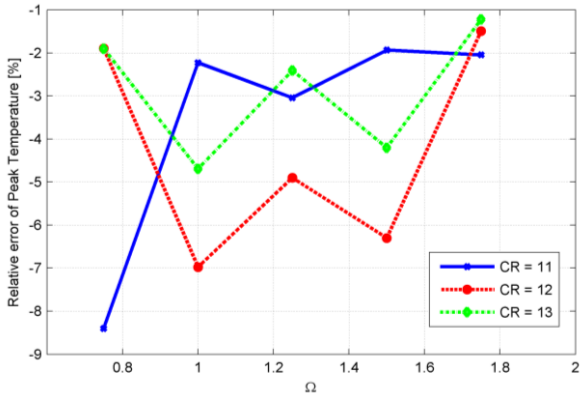

Figure 12. Relative error of peak temperature from the two models at various working conditions

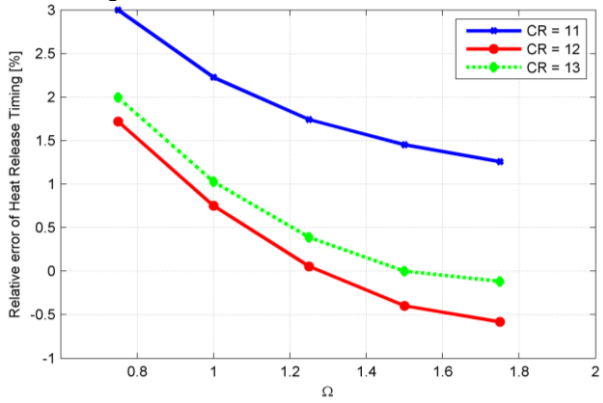

Figure 13. Relative error of time instants of heat release from the two models at various working conditions

Similarly, the fidelity of the proposed control-oriented model for the n-heptane at various working conditions is illustrated through the relative errors of the peak temperatures and the time instants of major heat release along different piston trajectories with various CR and Ω (Fig. 12 and Fig. 13).

As can be seen, the relative errors of the peak temperature for the n-heptane case are within the range of -1% to -9%, relatively larger than its counterparts for the methane case. However, the relative errors of the time instant of the major heat release are still small (3% to -1%). The simulation results show that even the chemical kinetics of the n-heptane is much more complex than the methane, the derived control-oriented model from this framework can still be accurate in terms of the prediction of the peak T and the heat releasing timing.

C. Bio-diesel

The bio-diesel is usually a combination of saturated methyl esters and saturated methyl esters. For the sake of the convenience, the formula of the bio-diesel in this study is assumed as the formula of the methyl decanoate, $C_{11}H_{22}O_2$, Therefore, the related chemical kinetics part can be refined as follow:

$$R_1 : C_{11}H_{22}O_2 + 4.5O_2 \rightarrow 11CO + 11H_2$$

and the corresponding production rate of each species in the ignition phase is:

$$\begin{cases} w_{C_{11}H_{22}O_2} = -RR_1 \\ w_{O_2} = -4.5RR_1 \\ w_{H_2} = 11RR_1 \\ w_{CO} = 11RR_1 \\ w_{CO_2} = 0 \\ w_{H_2O} = 0 \end{cases}$$

The final calibration results of the control-oriented model for the bio-diesel are listed in Table 8.

Table 8. Calibration result of the chemical kinetics parameters for the control-oriented model of bio-diesel

Parameters	*Value*
A_1	7.613e9
A_3	5.371e9
E_{A2}	15873
n_1	-0.17
n_2	2.53
n_6	1.07

I. Computational Cost

In this case, the detailed reaction-based model needs 6638ms to derive the final results, while the corresponding control-oriented model speeds up by 98.27%, only needs 115ms.

Table 9. Comparison of the computational times of the two models

Utilized model	Computational time [ms]
Detailed reaction-based model	6638
Proposed control-oriented model	115

II. Accuracy of the Prediction

In terms of the accuracy of the prediction, Fig. 14 shows the comparison of the *T* profiles between the two models for bio-diesel at a specific working condition (AFR = 2, CR = 23 and Ω = 0.75). As can be seen, the time instant of the start of combustion and the peak temperature have relatively larger errors as 2.00% and 1.90% respectively, compared to the aforementioned two cases.

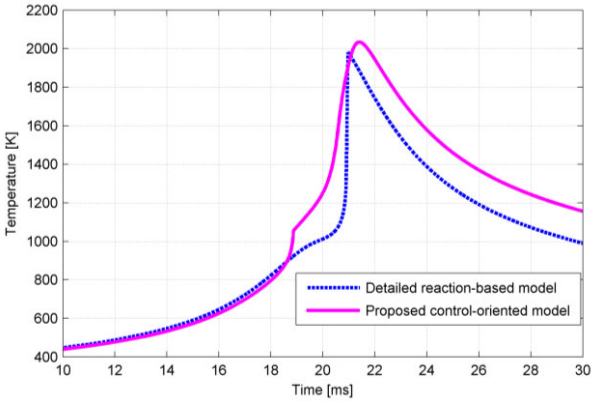

Figure 14. Comparison of temperature profiles between the two models (AFR = 2, CR = 23 and Ω = 0.75)

The relative errors of the peak *T* and the time instants of major heat release along various CRs and Ωs are shown in Fig. 15 and Fig. 16. The relative error of the peak *T* for the biodiesel case is within the range of 9% to -8% and the relative error of the heat release timing is within the range of 7% to -2%. Clearly, as the molecule structure of the fuel becomes more complex, the performance of the control-oriented model derived from the proposed framework is weakened

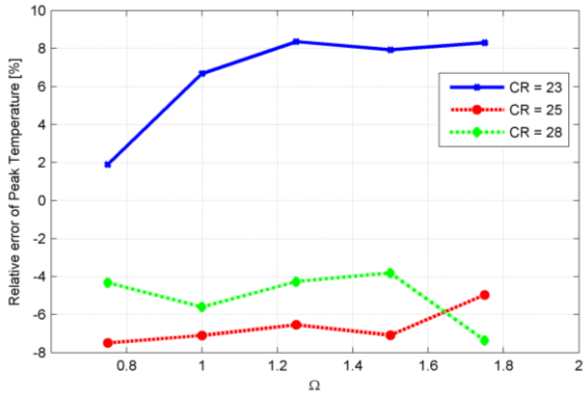

Figure 15. Relative error of peak temperature from the two models at various working conditions

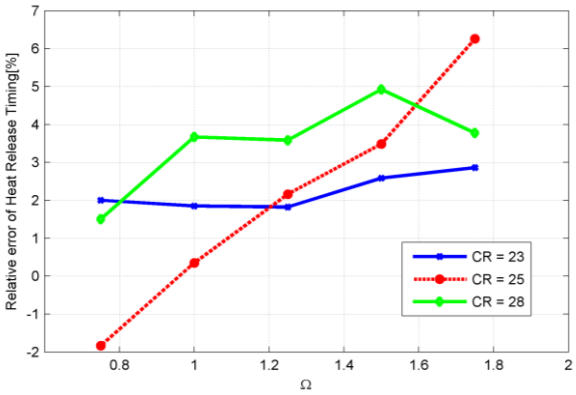

Figure 16. Relative error of time instants of heat release from the two models at various working conditions

CONCLUSION

In this paper, a framework of a new control-oriented model with a unique phase separation method is proposed to realize the trajectory-based HCCI combustion control for variable fuels. With the phase separation method, an engine cycle is separated into four phases and specific reaction mechanisms are employed accordingly to represent the chemical kinetics of the combustion process. In order to extend the framework to variable fuels, a model calibration method, based on the least-square optimization, is employed and critical chemical kinetics parameters are thus calibrated according to the related detailed reaction mechanisms. In this way, three control-oriented models, with the identical model structure but different values of the chemical kinetics parameters, are derived for methane, n-heptane, and bio-diesel respectively.

For the three fuels, the comparisons between their control-oriented models and the related detailed reaction-based models show a good agreement, in terms of in-cylinder *T* and NOx emissions. Such a good agreement is also sustained while simulating the HCCI combustion process along various piston trajectories with different CRs and Ωs. Besides, the proposed control-oriented models also increase their computational efficiency by 95% or more. On top of that, this computational advantage is even more significant while more complex fuels are investigated.

ACKNOWLEDGMENTS

The authors would like to thank the National Science Foundation (NSF) for the financial support under grant CMMI-1634894.

REFERENCES

[1] Onishi, S.,Han Jo, S., Shoda, K., Do Jo, P. and Kato, S., 1979, "Active Thermo-Atmosphere Combustion (ATAC): A New Combustion Process for Internal Combustion Engine," SAT Technical Paper Series, Paper NO. 790501

[2] Zhao, F., Asmus, T. W., Assanis, D. N, and Dec, J. E., 2003, "Homogeneous Charge Compression Ignitions (HCCI) Engines: Key Research and Development Issues," SAE International, PT-94

[3] Epping, K., Aceves, S., Bechtold, R. and Dec, J., 2002, "The Potential of HCCI Combustion for High Efficiency and Low Emissions," SAE Technical Paper 2002-01-1923

[4] Zhao, H., Peng, Z., Williams, J., Ladommatos, N., 2001, "Understanding the Effects of Recycled Gases on the Controlled Autoignition (CAI) Combustion in Four-Stroke Gasoline Engines." SAE Paper No.2001- 01-3607

[5] Ladommatos, N. Abdelhalim, S, and Zhao, H., 2000, "The Effects of Exhaust Gas Recirculation on Diesel Combustion and Emissions," Int. J. Engine. Res., **1**(1), pp. 107–126

[6] Caton, P. A., Songm H. H., Kaahaainam N. B. and Edwards, C. F., 2005, "Strategies for Achieving Residual-Affected Homogeneous Charge Compression Ignition using Variable Valve Actuation," SAE Paper NO. 2005-01-0165

[7] Law, D., Kemp, D., Allen, J., Kirkpatrick, G., and Copland, T., 2001, "Controlled Combustion in an IC-Engine with a Fully Variable Valve Train," SAE Paper No. 2001-01-0251

[8] Marriott, C. D and Reitz, R. D., 2002, "Experimental Investigation of Direct Injection Gasoline for Premixed Compression Ignited Combustion Phasing Control," SAE Paper NO. 2002-01-0418

[9] Sjoberg, M., Edling, L. O., Eliassen, T., Magnusson, L. and Angstrom, H. E., 2002, "GDI HCCI: Effects of Injection Timing and Air-Swirl on Fuel Stratification Combustion and Emissions Formation." SAE Paper NO. 2002-01-0106

[10] Zhang, C., Li, K. and Sun, Z., 2015, "Modeling of Piston Trajectory-based HCCI Combustion Enabled by a Free Piston Engine," Applied Energy, 139(1), pp. 313-326

[11] Zhang, C. and Sun, Z., 2016, "Using Variable Piston Trajectory to Reduce Engine-out Emissions," Applied Energy, 170(1), pp. 403-313

[12] Zhang, C. and Sun, Z., 2017, "Trajectory-based Combustion Control for Renewable fuels in Free Piston Engines," Applied Energy, 187(1), pp. 72-83

[13] Li, K., Sadighi, A. and Sun, Z., 2014, "Active Motion Control of a Hydraulic Free Piston Engine," IEEE/ASME Transaction. Mechatronics, 19(4), pp. 1148-1159

[14] Mikalsen, R. and Roskilly, A. P., 2007, "A Review of Free-piston Engine History and Applications," Applied Thermal Engineering, 27(14-15), pp.2339-2352

[15] Li, K., Zhang, C. and Sun, Z., 2015, "Precise Piston Trajectory Control for a Free Piston Engine," Control Engineering Practice, 34, pp. 30-38

[16] Zhang, C. and Sun, Z., 2016, "Optimization of Trajectory-based HCCI Combustion," Proceedings of Dynamic Systems Control Conference, Minneapolis MN, 2016

[17] Li, K. and Sun, Z., 2011, "Stability Analysis of a Hydraulic Free Piston Engine with HCCI Combustion," Proceedings of Dynamic Systems Control Conference, Arlington VA, 2011

[18] Shaver, G. M., Gerdes, J, C., Roelle, M. J., Caton, P. A. and Edwards, C. F, 2005, "Dynamic Modeling of Residual-affected Homogeneous Charge Compression Ignition Engines with Variable Valve Actuation," Journal of Dynamics Systems, Measurement and Control, 127, pp. 374-381

[19] Zhang, S., Song, R. and Zhu, G. G., 2017, "Model-based Control for Model Transition Between Spark Ignition and HCCI Combustion," Journal of Dynamics Systems, Measurement and Control, 139(4), 041004

[20] Shahbakhti, M. and Koch, C. R., 2010, "Physics Based Control Oriented Model for HCCCI Combustion Timing," Journal of Dynamics Systems, Measurement and Control, 132(2), 021010

[21] Zhang, C. and Sun, Z., 2015, "A Control-oriented Model for Piston Trajectory-based HCCI Combustion," Proceedings of American Control Conference, Chicago, IL, 2015

[22] J. Heywood, 1988, Internal Combustion Engine Fundamentals, McGraw-Hill

[23] Goodwin, D., Malaya N. and Speth. R., "Cantera: An Object-oriented Software for Chemical Kinetics, Thermodynamics and Transport Processes", available at https://code.google.com/p/cantera/

[24] Zeldovich, Y. A., Frank-Kamenetskii, D. and Sadovnikov, P., 1947, "Oxidation of Nitrogen in Combustion," Publishing House of the Academy of Sciences of USSR

[25] Bowman, C. T., 1975, "Kinetic of Pollutant Formation and Destruction in Combustion," Progress in Energy Combust. Sci., 1(1), pp. 33-45

[26] Hamby, D., 1994, "A Review of Techniques for Parameter Sensitivity Analysis of Environmental Models," Environmental Monitoring and Assessment, 32(2), pp.135-154

[27] Jones, W. P. and Lindstedt, R. P., 1988, "Global Reaction Schemes for Hydrocarbon Combustion," Combustion and Flame, 73(3), pp. 233-249

[28] Coleman T. F. and Li, Y., 1996, "An Interior Trust Region Approach for Nonlinear Minimization Subject to Bounds," SIAM Journal on Optimization, 6(2), pp. 418-445

[29] Pachner, D., Germann, D. and Stewart, G., 2012, "Identification Techniques for Control Oriented Models of Internal Combustion Engines," In Identification for Automotive Systems, pp. 257-282, Springer London.